

Ultrathin Colloidal PbS/CdS Core/Shell Nanosheets

Simeen Khan,¹ Zhoufeng Jiang,^{1,2} Shashini M Premathilka,^{1,2} Jianjun Hu,³ Andrey Voevodin,³ Paul J. Roland,⁴ Randy J. Ellingson,⁴ Liangfeng Sun^{1,2}

¹Department of Physics and Astronomy, Bowling Green State University, Bowling Green, OH 43403, USA

²Center of Photochemical Sciences, Bowling Green State University, Bowling Green, OH 43403, USA

³Materials and Manufacturing Directorate, Air Force Research Laboratory, Wright-Patterson Air Force Base, OH 45433, USA

⁴Department of Physics and Astronomy, Wright Center for Photovoltaics Innovation and Commercialization, School of Solar and Advanced Renewable Energy, University of Toledo, Toledo, Ohio 43606, USA

ABSTRACT

Emissive PbS/CdS core/shell nanosheets are synthesized using a cation-exchange method. A significant blue-shift of the photoluminescence is observed, indicating a stronger quantum confinement in the PbS core as its thickness is reduced to eight atomic layers. High resolution transmission-electron-microscopy images of the cross-sections of the core/shell nanosheets show atomically sharp interfaces between PbS and CdS. Accurate analysis of the thickness of each layer reveals the relationship between the energy-gap and the thickness in the extremely one-dimensionally confined nanostructure.

INTRODUCTION

Quantum confinement is the origin of the novel properties of quantum dots. However, three-dimensional confinement also hinders the charge transfer among the quantum dots, which limits the performance of the quantum-dot-based electronic devices. In a two-dimensional (2D) structure, the charges within the 2D plane have high charge mobilities^{1, 2} while the one-dimensional quantum confinement is retained in the thickness direction. Consequently, the tunable optical properties and the high charge mobility are unified in a single structure. Fabrication of these 2D materials using epitaxial methods is challenging due to the lack of lattice matching substrates.^{3, 4} A wet-chemistry synthesis of colloidal nanosheets^{1, 5-11} provides an alternative solution. The synthesized colloidal nanosheets are counterparts of the epitaxial quantum wells,¹² but are free-standing and low-cost (since no high-vacuum or high-temperature is needed for the synthesis).¹³ We report a facile synthesis of emissive PbS/CdS core/shell nanosheets using cation-exchange methods. Significant blue-shift of the photoluminescence peak is observed, indicating stronger quantum confinement in the PbS core with reduced thickness. High resolution transmission electron microscopy (HRTEM) images of the cross-section of the nanosheets show clear crystal interfaces between PbS and CdS.

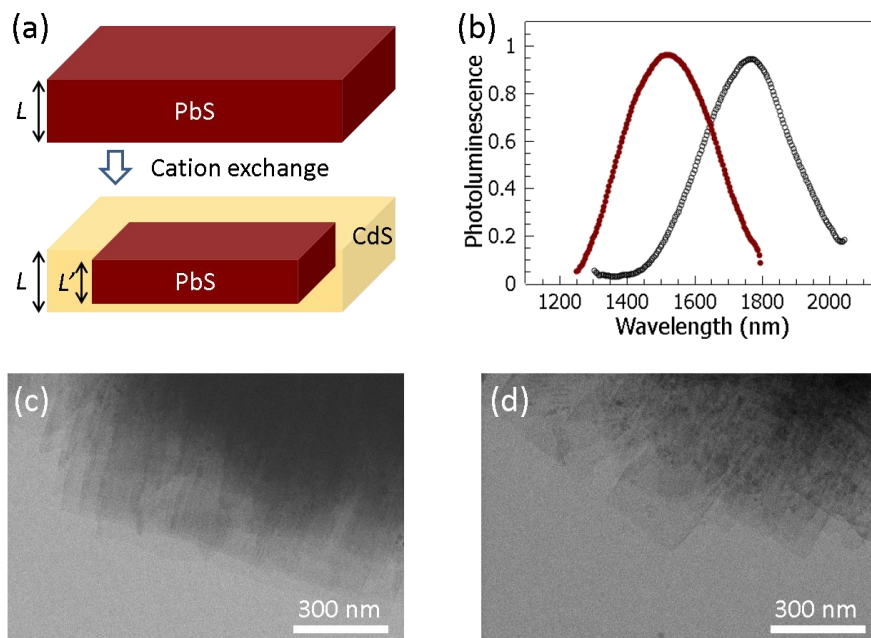


Figure 1. (a) Scheme showing the process of cation exchange for PbS/CdS structure. The overall dimension of the sheet remains the same while the out-layers of the material turn into CdS. (b) Photoluminescence spectra from the nanosheets before (open circles) and after (solid circles) cation exchange showing the shift of the peak from 1760 nm to 1520 nm. (c) TEM image of the stacked original PbS nanosheets. Each nanosheet has a lateral size of a few hundred nanometers. (d) TEM image of the stacked nanosheets after cation exchange showing a similar morphology as in (c).¹⁴

EXPERIMENT

The synthesis of PbS nanosheets is based on the methods invented by Weller's group⁶ and developed by others.^{1, 15} After PbS nanosheets are synthesized and purified, a cation-exchange method^{16, 17} is used to exchange the outer layer Pb ions with Cd ions to form a CdS shell surrounding the PbS core. In brief, cadmium oxide is mixed with oleic acid and heated under nitrogen to form cadmium oleate, which is then mixed with PbS nanosheets for the cation-exchange reaction. The reaction is stopped by adding cold hexane. The final solution is washed twice with toluene and finally dispersed in toluene. This method does not change the overall thickness of the nanosheets but rather reduces the thickness of PbS core (Figure 1a).

The transmission electron microscopy (TEM) images (Figure 1c, d) and secondary-electron images show that the morphology of the nanosheets remains the same after cation exchange. However, there is a significant blue-shift (Figure 1b) of the photoluminescence indicating the decrease of the thickness of the PbS core. Further energy-dispersive X-ray spectroscopy measurements show a clear Cd peak after cation exchanges.

To learn the details of the heterostructure formed in PbS/CdS nanosheets, it is essential to prepare the nanosheets standing on edge so that the cross-sections of the nanosheets can be imaged using HRTEM. To achieve this goal, small-lateral-size nanosheets having width around 20 nm are synthesized. The narrow width of the nanosheet makes it easy for them to stand up on the TEM substrate (Figure 2a). The HRTEM image (Figure 2b) shows an array of dots which is the projection of the ions in the nanosheets onto the substrate. This image reveals that the

surfaces of the nanosheets are atomically flat. The standing-up PbS nanosheets shows a single-crystal structure with 12 atomic layers in the thickness direction. The thickness can be calculated through multiplying the lattice constant of PbS ($c=0.594\text{ nm}$) by the multiple of lattice constant the thickness spans (5.5), resulting in a thickness determination in this case of 3.27 nm . This thickness matches that obtained ($3.3 \pm 0.1\text{ nm}$) using the calibrated HRTEM instrument. The dependence of the energy gap on the thickness of the PbS nanosheets is still under debate,^{6, 15, 18} partially due to the difficulty on the thickness measurements. Since the nanosheets can be prepared standing-up on the substrate, their thickness can be accurately measured without ambiguity.

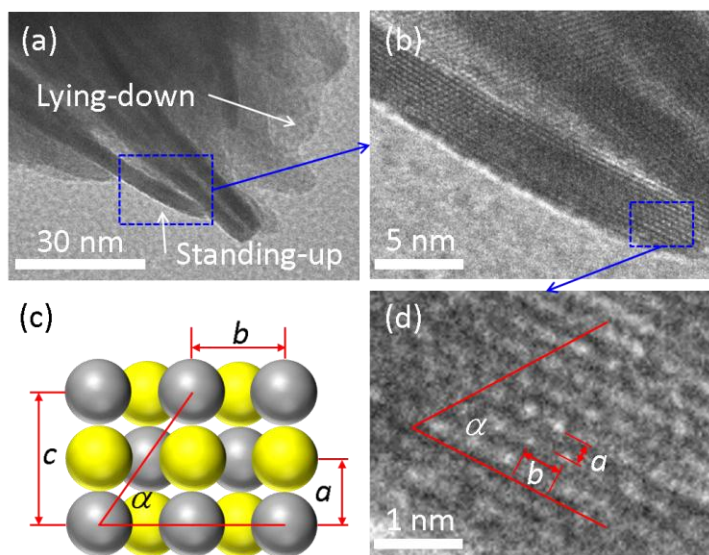


Figure 2. (a) A TEM image of PbS nanosheets showing both standing-up and lying-down nanosheets. (b) The close-up HRTEM image of one standing-up nanosheets shows a single-crystalline structure with 12 layers of ions in the thickness direction. (c) Diagram showing the arrangement of the ions viewed in $\langle 110 \rangle$ direction of the crystal. (d) In the thickness direction, the spacing between the neighbor ions a is 0.297 nm , while in the orthogonal direction, the spacing between the neighbor ions b is 0.42 nm . The angle α is about 55° .¹⁴

All of the observed cross-sections of the nanosheets show the same facet as in Figure 2b. For the projection of $\{110\}$ facet of PbS crystal (Figure 2d), the spacing between neighbor ions in $\langle 001 \rangle$ direction is $a = c/2 = 0.297\text{ nm}$, while the spacing between the neighbor ions (within the same plane) in the orthogonal direction $\langle 110 \rangle$ is $b = c/\sqrt{2} = 0.420\text{ nm}$. The angle α (Figure 2d) between the line of the same ions and $\langle 110 \rangle$ direction is then 55° . All of the parameters a , b and α as measured using HRTEM (Figure 2c) match up with the calculated results above. This confirms the observed surface of the nanosheet edge has a $\{110\}$ facet and the top/bottom surfaces of the nanosheet have a $\{001\}$ facet. This result is consistent with the earlier 2D oriented attachment model¹⁹ for the growth mechanism of 2D PbS nanosheets, i.e., the PbS quantum dots attach to each other through $\{110\}$ facets, resulting in $\{110\}$ facets at the edges of the nanosheets.

The same PbS nanosheets are used to synthesize PbS/CdS core/shell nanosheets. After cation exchange, the core/shell nanosheet shows atomically sharp interfaces between PbS and CdS (Figure 3). The PbS core has about 8 atomic layers, indicating ~ 2 atomic layers of PbS have been turned into CdS on each side of the nanosheet, reducing the thickness of the PbS core to 2.1

nm as measured with HRTEM. The HRTEM image (Figure 3) of the cross-section of the PbS/CdS nanosheet shows a {110} facet as in the original PbS nanosheet (Figure 2c). At some locations the crystal structure of the CdS shell remains nearly the same as the PbS core (Figure 3b) as in the case of core/shell PbS/CdS quantum dots,²⁰ while it appears amorphous at other locations. The PbS/CdS heterostructure is clearly revealed by the sharp contrast in the HRTEM image, which is due to the high atomic-weight ratio Pb/Cd.

The interfaces between PbS and CdS are atomically flat, indicating that the cation exchange occurs uniformly from the surface into the bulk of the nanosheet. This differs from what was observed in PbSe/CdSe nanorods,²¹ for which a zigzag shaped core terminated by {111} interfaces forms. The reaction temperature is believed to play a key role in achieving uniform cation exchange. On the other hand, smaller surface to volume ratio in 2D sheets in contrast to 1D nanorods likely favor a uniform cation-exchange. Similar work by Dubertret and coworkers demonstrated that flat interfaces formed after cation-exchanges in PbS/CdS, CdSe/CdS and ZnSe/ZnS nanoplatelet.²²

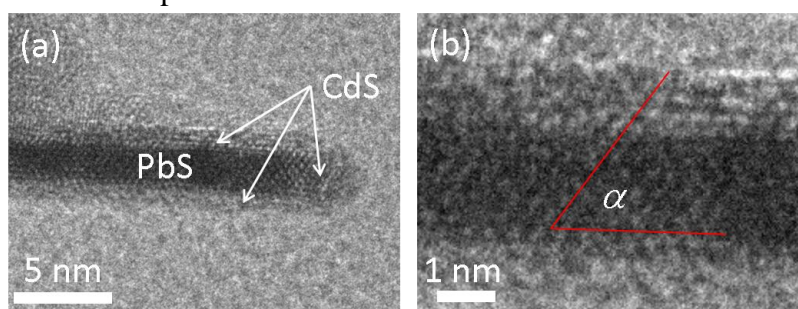


Figure 3. (a) HRTEM image showing atomically sharp interfaces between the PbS core and the CdS shell. (b) Zoomed-in HRTEM image showing the similar crystal structure of the CdS shell as the PbS core. The lines are to guide the eyes to the array of ions, making the angle α unique to {110} facet as mentioned earlier.¹⁴

The element mapping of the vertically aligned PbS/CdS core/shell nanosheets shows the same image for Pb, Cd and S elements, and each of them overlaps with the high-angle-annular-dark-field image. It reveals that the cation exchange occurs uniformly. At this time, the resolution of the element mapping is not high enough to map out the elements layer by layer, but the element analysis over the ensemble of the nanosheets shows the molar ratio of lead (Pb) to cadmium (Cd) is around 2.4:1. It is consistent with the HRTEM analysis: around 8 layers of PbS versus 4 layers of CdS.

The PbS/CdS nanosheets fluoresce in the infrared as the original PbS nanosheets,¹⁵ in contrast to non-emissive ZnSe/ZnS and PbSe/PbS core/shell nanoplatelets.²² Those nanoplatelets were created using two-step cation-exchange – CdSe/CdS to Cu₂Se/Cu₂S then to ZnSe/ZnS or PbSe/PbS. The excess trap sites formed by the residue copper atoms were thought to quench the photoluminescence.²² The emissive nanosheets help to determine the optical energy gap, given the fact that the Stokes' shift is negligible for PbS nanosheets.¹⁵ The photoluminescence of the core/shell nanosheets shows a significant blue-shift as compared with the original PbS nanosheets (Figure 4a), indicating stronger quantum confinement due to the decrease of the core thickness after cation exchange. The photoluminescence shift mainly occurs within 15 minutes after reaction. The shift is negligible beyond 15 minutes, indicating that the cation-exchange process is self-limiting under the reaction conditions used (Figure 4a). The optical energy gaps obtained from photoluminescence spectroscopy and the thicknesses obtained using HRTEM are

plotted together in Figure 4b. The data points are slightly above the fitting curve obtained previously.¹⁵ The slightly-larger energy gap is likely due to the additional confinement in the width direction since the width of the nanosheets is about 20 nm which is close to the exciton Bohr radius of PbS. In the core/shell structure, the wave function of the charge carrier in the PbS core extends into the CdS shell, resulting less quantum confinement.²³ Consequently, the PbS nanosheet without CdS shell has a slight larger energy gap than the PbS core with the same thickness but capped by a CdS shell. As expected, the confinement energy in either the PbS nanosheets or PbS/CdS core/shell nanosheets is much less than in quantum-dots with the diameter equal to the thickness of the nanosheets. This is mainly due to the difference of 3D confinement (QDs) and 1D confinement (nanosheets).¹⁵

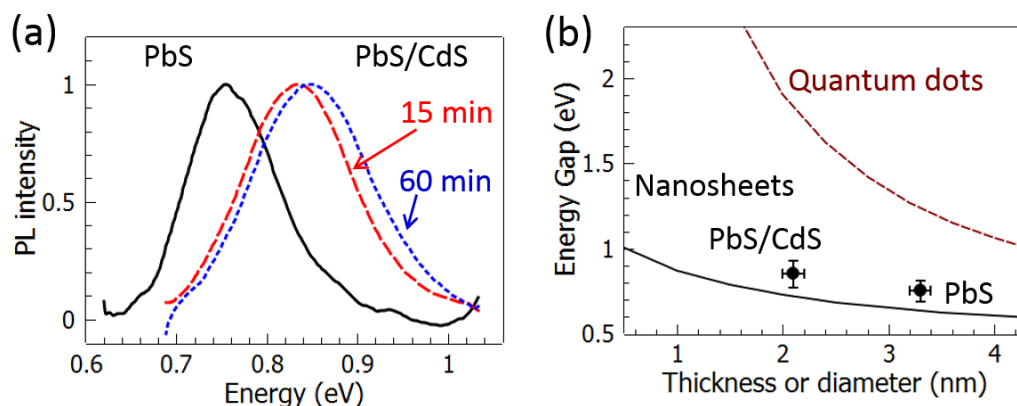


Figure 4. (a) The photoluminescence peak shifts from 0.75 eV to 0.83 eV and 0.85 eV after 15 minutes (dashed line) and 60 minutes (dotted line) cation exchanges, respectively. (b) The energy-gap dependence on the thickness follows the $1/L$ (L is the thickness of the PbS layer) model (solid line)¹⁵ for both PbS nanosheets and PbS/CdS core/shell nanosheets. The increase of the energy gap of PbS quantum dots (dashed line)²⁴ is much faster than the nanosheets as the diameter decreases.¹⁴

CONCLUSIONS

In summary, a facile synthesis of PbS/CdS core/shell nanosheets is developed. The core/shell heterostructure synthesized using cation-exchange methods has an increased energy gap. Proper preparations of standing-up nanosheets enable accurate characterizations of the core/shell crystal structures as well as their thicknesses. The HRTEM reveals that the interface between PbS and CdS is nearly atomic flat. It is expected this method can be used to create thinner (less than 8 atomic layers) PbS sheets capped by CdS using thinner original PbS nanosheets and/or adjusting the reaction conditions.

ACKNOWLEDGMENTS

The work is partially supported with funding provided by the Office of the Vice President for Research & Economic Development, Bowling Green State University. L. Sun thanks the funding provided by the U.S. Air Force Research Lab Summer Faculty Fellowship Program. We thank Charles Coddling (machine shop) and Doug Martin (electronic shop) for their technical assistance at BGSU. The authors thank Joseph G. Lawrence for his help on the TEM measurements at the University of Toledo. P. Roland and R. Ellingson gratefully acknowledge

support of the Air Force Research Laboratory under contracts FA9453-08-C-0172 and FA9453-11-C-0253. R. Ellingson acknowledges additional support from startup funds provided by the Wright Center for Photovoltaic Innovation and Commercialization.

REFERENCES

1. Dogan, S., Bielewicz, T., Cai, Y. & Klinke, C. *Appl. Phys. Lett.* **101**, 073102 (2012).
2. Dogan, S., Bielewicz, T., Lebedeva, V. & Klinke, C. *Nanoscale* **7**, 4875 (2015).
3. Dasgupta, N. P., Lee, W. & Prinz, F. B. *Chem. Mater.* **21**, 3973 (2009).
4. Dasgupta, N. P., Wonyoung Lee, Holme, T. P. & Prinz, F. B. *Atomic Layer Deposition of PbS-ZnS quantum wells for high-efficiency solar cells* (Photovoltaic Specialists Conference (PVSC), 2009 34th IEEE, 2009).
5. Acharya, S., Sarma, D. D., Golan, Y., Sengupta, S. & Ariga, K. *J. Am. Chem. Soc.* **131**, 11282 (2009).
6. Schliehe, C. *et al. Science* **329**, 550 (2010).
7. Acharya, S. *et al. Nano Lett.* **13**, 409 (2013).
8. Joo, J., Son, J. S., Kwon, S. G., Yu, J. H. & Hyeon, T. *J. Am. Chem. Soc.* **128**, 5632 (2006).
9. Ithurria, S. & Dubertret, B. *J. Am. Chem. Soc.* **130**, 16504 (2008).
10. Son, J. *et al. Angewandte Chemie International Edition* **48**, 6861 (2009).
11. Ithurria, S. *et al. Nature Materials* **10**, 936 (2011).
12. van der Ziel, J. P., Dingle, R., Miller, R. C., Wiegmann, W. & Nordland, W. A. *Appl. Phys. Lett.* **26**, 463 (1975).
13. Yang, J., Son, J. S., Yu, J. H., Joo, J. & Hyeon, T. *Chem. Mater.* **25**, 1190 (2013).
14. Khan, S. *et al. Chem. Mater.* **28**, 5342 (2016).
15. Bhandari, G. B. *et al. Chem. Mater.* **26**, 5433 (2014).
16. Pietryga, J. M. *et al. J. Am. Chem. Soc.* **130**, 4879 (2008).
17. Moroz, P. *et al. Chem. Mater.* **26**, 4256 (2014).
18. Aerts, M. *et al. Nat Commun* **5**, 3789 (2014).
19. Jiang, Z. *et al. Phys. Chem. Chem. Phys.* **17**, 23303 (2015).
20. Lechner, R. T. *et al. Chem. Mater.* **26**, 5914 (2014).
21. Casavola, M. *et al. Chem. Mater.* **24**, 294 (2012).
22. Bouet, C. *et al. Chem. Mater.* **26**, 3002 (2014).
23. Bartnik, A. C., Wise, F. W., Kigel, A. & Lifshitz, E. *Phys. Rev. B* **75**, 245424 (2007).
24. Moreels, I. *et al. ACS Nano* **3**, 3023 (2009).